PHYSICAL REVIEW E VOLUME 49, NUMBER 6 JUNE 1994

Nature of the layer-by-layer transition associated with the smectic-A–crystal-B transition in free-standing liquid-crystal films

A. J. Jin, T. Stoebe, and C. C. Huang
School of Physics and Astronomy, University of Minnesota, Minneapolis, Minnesota 55455
(Received 10 March 1994)

Utilizing our ac free-standing film calorimeter, we have observed the formation of a series of crystal-B layers at the smectic-A–vapor interface near the smectic-A–crystal-B transition of 4O.8 [N-(4-n-butyloxybenzylidene)-4-n-octylaniline]. The temperature dependence of the penetration of the crystal-B order into the smectic-A substrate can be well described by a simple power law, $L = L_0|t|^{-\nu}$ with $\nu = 0.37$, indicating that the dominant intermolecular interaction is van der Waals like. Further analysis has demonstrated the penetration length of the surface ordering to be slightly less than one molecular length.

PACS number(s): 64.70.Md, 61.30.−v, 68.65.+g

Detailed x-ray investigations [1–3] have revealed two distinct orthogonal liquid-crystal phases below the smectic-A (Sm-A) phase, namely, the hexatic-B (Hex-B) and crystal-B (Cry-B) phases. The Sm-A–Hex-B transition has been observed in several members of the nmOBC homologous series (n-alkyl-4′-n-alkyloxybiphenyl-4-carboxylate) [1]. However, the transition near 49 °C of the compound 4O.8 [N-(4-n-butyloxybenzylidene)-4-n-octylaniline] has been identified as the Sm-A–Cry-B [2,3]. The Hex-B and Cry-B phases can be distinguished by the extent of positional order. Unlike the Hex-B phase, the Cry-B phase exhibits three-dimensional long-range positional order. Furthermore, according to the symmetry of the order parameter associated with the given transition, the bulk Sm-A–Cry-B transition is required to be first order, while the Sm-A–Hex-B transition in nmOBC compounds is found to be continuous [4]. High-resolution x-ray-diffraction studies [2,3] of 4O.8 free-standing films in the Cry-B phase have, in fact, revealed both interlayer and intralayer long-range positional order. Furthermore, the Cry-B phase is optically uniaxial since the molecules remain free to rotate around their long axes, which are, on average, parallel to the layer normal. Calorimetric investigations of bulk samples have observed a hysteretic, broad heat-capacity peak, indicative of the first-order nature of the Sm-A–Cry-B transition [4,5]. Recently, we have identified and characterized a unique layer-by-layer transition associated with the continuous Sm-A–Hex-B transition in 3(10)OBC films, indicating strong surface ordering effects and weak interlayer coupling. Before this work, layer-by-layer transitions had been theoretically addressed and experimentally investigated near first-order transitions only. Based on symmetry arguments, transitions establishing long-range positional order in three dimensions are expected to be first order. Although surface enhanced crystalline order has been observed in several liquid-crystal compounds [6–8], to the best of our knowledge, no layer-by-layer transition involving crystalline order has been previously reported. In this paper we will report the observation of a sequence of layer-by-layer transitions found near the Sm-A–Cry-B transition of 4O.8 free-standing liquid-crystal films.

So far, layer-by-layer transitions in liquid crystals have been identified near the isotropic–Sm-A [9], Sm-A–smectic-I (Sm-I) [10], and Sm-A–Hex-B [11] transitions. The first two cases involve first-order transitions, while the last is a continuous transition. However, none of the above liquid-crystal mesophases exhibits long-range positional order. The sequences of layer-by-layer transitions near both the Sm-A–Sm-I and Sm-A–Hex-B transitions were found to be well described by a power law obtained from a simple wetting calculation, assuming the system is dominated by van der Waals forces. Similarly, the layer-by-layer surface crystallization reported here can be characterized by the same power-law form, indicating that van der Waals forces are again dominant in this case. Further data analyses have also demonstrated the penetration length to be slightly less than one molecular layer, consistent with the layer-by-layer nature of the transition.

We have recently established a state-of-the-art differential ac calorimetric system which enables us to simultaneously measure the temperature dependence of the heat capacity and optical reflectivity of free-standing liquid-crystal films down to only two molecular layers in thickness [12–14]. The relative resolution of both heat-capacity and optical reflectivity measurements is better than a few parts in 10^5. Employing this unique calorimeter, we have conducted detailed heat-capacity measurements on free-standing 4O.8 films as a function of film thickness near the Sm-A–Cry-B transition. The data from 3-, 4-, 5-, and 25-layer films are shown in Fig. 1. It is clear that the surface transition temperature (approximately 62 °C) is enhanced significantly above the bulk transition temperature (about 49 °C). This 13 K increase in transition temperature and the long-range positional order of the Cry-B phase may be the primary reason that two-layer films easily rupture once cooled through the surface Sm-A–Cry-B transition. As the film establishes Cry-B order, the sample at the edge of the film plate remains in the Sm-A phase. Thermal contraction may then cause the two-layer films to become extremely fragile. Consequently, despite many experimental attempts,

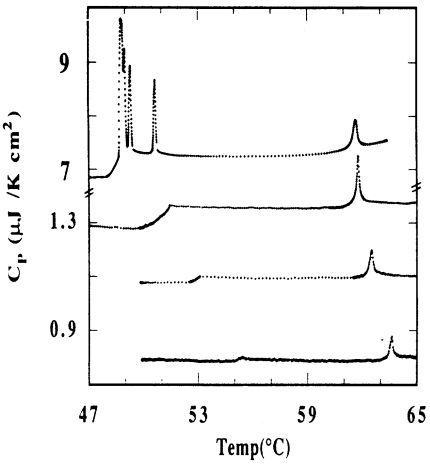

FIG. 1. Heat-capacity data from 3-, 4-, 5-, and 25-layer films of 4O.8 near the Sm-A–Cry-B transition. Note: the vertical scale for the 25-layer film has been reduced.

two-layer film data could not be obtained.

The surface Sm-A–Cry-B transition (see Fig. 1) displays a very different heat-capacity anomaly than that associated with the surface Hex-B–crystal-E (Cry-E) transition of 75OBC [7,14] or 65OBC [15]. The latter transition appears as an abrupt heat-capacity jump and exhibits substantial thermal hysteresis. Furthermore, it does not occur in a layer-by-layer fashion [16]. The series of transitions shown in Fig. 1 are also distinctly different from those observed near the Sm-A–Hex-B transition. For $N \geq 3$, the freezing transition of the outermost surface layers occurs on the liquidlike interior Sm-A layer(s). This represents a two-dimensional liquid-to-crystalline transition on a liquidlike "substrate." The presence of this "substrate" is most likely the major reason that significant pretransitional behavior associated with the Sm-A–Cry-B transition of the outermost layers can be detected. In the case of the continuous Sm-A–Hex-B transition, the size of the surface heat-capacity anomaly is independent of film thickness [14]. Figure 1 indicates that the magnitude of the surface Sm-A–Cry-B heat-capacity peak increases as a function of the film thickness. (Note, the vertical scale has been reduced for the 25-layer film.) Successive heating and cooling runs have demonstrated thermal hysteresis to be less than 30 mK. However, attempts to fit the data to a simple power-law form ($C_p \approx t^{-\nu}$) failed. The transition related to the interior layer ordering of three-, four-, and five-layer films appears only as a change in slope of the heat capacity as a function of temperature. Simultaneous optical reflectivity measurements on five-layer films clearly resolve three separate transitions corresponding to the freezing of the outermost pair, adjacent pair, and innermost layer. In the case of the 25-layer film, a symmetric heat-capacity peak again signals the surface freezing transition. The rest of the heat-capacity anomalies appear as much sharper peaks with lessened pretransitional contributions. Thus, under the influence of the surface ordering field, the interior layers possess a very different thermal signal than the outermost surface layers. After six distinct pairs of layer transitions, the interior 13 layers undergo a transition without displaying an additional heat-capacity anomaly. To illustrate this observation, Fig. 2 shows the simultaneous heat-capacity and optical reflectivity data obtained from an eight-layer film. The heat-capacity data display two well-defined peaks and one hump. Upon cooling, the optical reflectivity data exhibit four distinct anomalies. The first three coincide perfectly with the corresponding heat-capacity anomalies. The fourth reflectivity anomaly should then

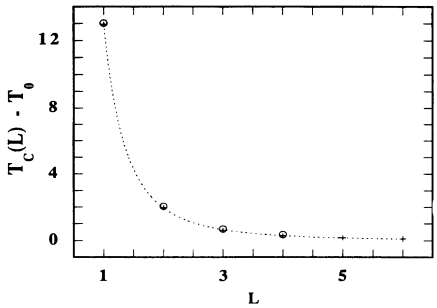

FIG. 3. Temperature $[T_c(L) - T_0]$ versus the penetration depth of the surface Cry-B phase (in layers, L). The dashed line is the best fit to the simple power law, $L = L_0\{[T_c(L) - T_0]/T_0\}^{-\nu}$. As expected, the resultant value for T_0 is roughly equal to the bulk Sm-A–Cry-B transition temperature.

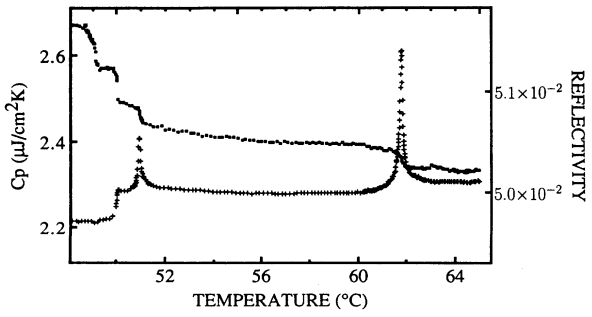

FIG. 2. Temperature variation of heat capacity and optical reflectivity simultaneously obtained from an eight-layer 4O.8 film. Note: the transition associated with the innermost two layers can be clearly seen in the optical reflectivity data but not in the heat-capacity data.

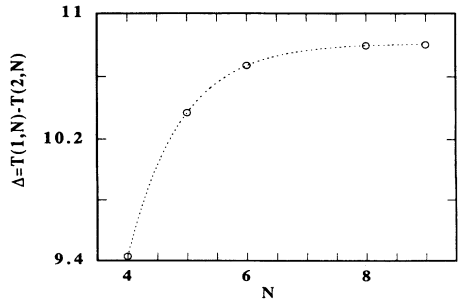

FIG. 4. The temperature difference $[\Delta = T(1,N) - T(2,N)]$ versus film thickness (N). The dashed line is the best fit of the data to the exponential form [Eq. (1)].

TABLE I. Transition temperatures (in °C) of different layers (L) in films 25 and 15 layers thick.

Thickness	$T_c(L=6)$	$T_c(L=5)$	$T_c(L=4)$	$T_c(L=3)$	$T_c(L=2)$	$T_c(L=1)$
25	48.71	48.74	48.93	49.24	50.59	61.60
15			48.94	49.27	50.63	61.60

signal the Sm-A–Cry-B transition of the innermost two layers, a transition absent from the heat-capacity data. In principle, by increasing the film thickness, more individual layer transitions should be able to be resolved. Unfortunately, the sensitivity of the optical reflectivity experiment decreases rapidly as the film thickness is increased. Furthermore, because of the finite width of the heat-capacity anomalies, the maximum experimental resolution occurs for $N \approx 25$.

Table I summarizes the transition temperatures for each identifiable layer transition of the 15- and 25-layer films. For comparison, bulk samples of 4O.8 display the following transition sequence [5]: isotropic(I) $\xrightarrow[78°\,\mathrm{C}]{}$ nematic(N) $\xrightarrow[64°\,\mathrm{C}]{}$ Sm-A $\xrightarrow[49°\,\mathrm{C}]{}$ Cry-B.

In the case of the 15-layer film, four separate heat-capacity peaks can be clearly identified. For 25-layer films, we can resolve six heat-capacity anomalies. This suggests that the transition may be an example of incomplete wetting. The data from 15- and 25-layer films are shown in Fig. 3. They can be well described by the simple power-law form [17], $L = L_0\{[T_c(L) - T_0]/T_0\}^{-\nu}$. The fitting results shown as the dashed line in Fig. 3 yield $\nu = 0.36 \pm 0.02$ and $L_0 = 0.32 \pm 0.01$. These values are quite similar to those found near the Sm-A–Sm-I transition ($\nu = 0.37$ and $L_0 = 0.24$) of 9O.4 [10] and the Sm-A–Hex-B transition ($\nu = 0.32$ and $L_0 = 0.31$) of 3(10)OBC [11]. Systems dominated by van der Waals forces are expected to be characterized by the exponent $\nu = \frac{1}{3}$. Intuitively, the value of L_0 should be related to some characteristic length scale. It is therefore interesting to note the strong agreement between the values of L_0 obtained from the purely orthogonal transitions while L_0 is significantly smaller in the transition that establishes a considerable molecular tilt (thereby reducing the characteristic layer spacing).

Table II displays the transition temperature, $T_c(1,N)$, of the outermost layers and that of the layers immediately adjacent to the surface layers, $T_c(2,N)$, as a function of film thickness N. From the table it is clear that $T_c(1,N)$ and $T_c(2,N)$ increase at different rates as film thickness decreases. The difference leads to a systematic variation of $\Delta T_c(N) = T_c(1,N) - T_c(2,N)$. The $\Delta T_c(N)$ versus film thickness data are presented in Fig. 4. The value of ΔT_c increases rapidly for small N and reaches an asymptotic value for $N \geq 8$. To a good approximation, the data can be described by the following simple expression (for $9 \geq N \geq 4$):

$$\Delta T_c(N) = \Delta T_0 - \delta T \exp(-N/\xi), \tag{1}$$

with $\Delta T_0 = 10.8$ K, $\xi = 0.87$, and $\delta T = 135$ K. Thus the effective penetration length of the surface ordering, ξ, is slightly less than one molecular layer, consistent with the observed layer-by-layer nature of the transition. The three-layer film data do not follow the above relation, however. Because the interior layer is immediately adjacent to the ordering field produced by both surface layers, the interior transition of the three-layer film could be expected to be significantly enhanced. To our surprise, the three-layer film exhibits a larger value of $\Delta T_c(3)$ (= 8.2 K) than that [$\Delta T_c(3)_{\mathrm{calc}} = 6.5$ K] extrapolated from Eq. (1). The observed depression of the interior layer transition temperature may be related to the energy barrier associated with the need to correlate the possibly unaligned Cry-B axes between the two surface layers and throughout the film.

In summary, the Sm-A–Cry-B transition in the 4O.8 free-standing films has been found to occur in a layer-by-layer fashion which is well characterized by a simple power-law expression derived from van der Waals forces. The effect of the ordered layers on the adjacent layers can be described by an exponential form with a characteristic length slightly less than one molecular length. The experimental investigation of other liquid-crystal compounds and phase transitions to acquire further physical insight into the nature of layer-by-layer transitions is in progress.

This work was supported in part by the National Science Foundation, Solid State Chemistry, Grant No. DMR93-00781.

TABLE II. Surface [$T(1,N)$] and next-to-surface transition temperatures [$T(2,N)$] (in °C) of various film thicknesses. $\Delta = T(1,N) - T(2,N)$.

Thickness	$T(1,N)$	$T(2,N)$	Δ
3	63.63	55.41	8.22
4	62.52	53.09	9.43
5	61.79	51.42	10.37
6	61.87	51.20	10.67
8	61.70	50.91	10.79
9	61.62	50.82	10.80

[1] R. Pindak, D. E. Moncton, S. C. Davey, and J. W. Goodby, Phys. Rev. Lett. **46**, 1135 (1981).
[2] D. E. Moncton and R. Pindak, Phys. Rev. Lett. **43**, 701 (1979).
[3] P. S. Pershan, G. Aeppli, J. D. Litster, and R. J. Birgeneau, Mol. Cryst. Liq. Cryst. **67**, 205 (1981).
[4] C. C. Huang, J. M. Viner, R. Pindak, and J. W. Goodby, Phys. Rev. Lett. **46**, 1289 (1981).
[5] K. J. Lushington, G. B. Kasting, and C. W. Garland, J. Phys. Lett. (Paris) **41**, L-419 (1980).
[6] R. Pindak, D. J. Bishop, and W. O. Sprenger, Phys. Rev. Lett. **44**, 1461 (1980).
[7] D. J. Bishop, W. O. Sprenger, R. Pindak, and M. E. Neubert, Phys. Rev. Lett. **49**, 1861 (1982).
[8] R. Geer, T. Stoebe, C. C. Huang, R. Pindak, G. Srajer, J. W. Goodby, M. Cheng, J. T. Ho, and S. W. Hui, Phys. Rev. Lett. **66**, 1322 (1991).
[9] B. M. Ocko, A. Braslau, P. S. Perhan, J. Als-Nielson, and M. Deutsch, Phys. Rev. Lett. **57**, 94 (1986).
[10] B. D. Swanson, H. Stragier, D. J. Tweet, and L. B. Sorenson, Phys. Rev. Lett. **62**, 909 (1989).
[11] T. Stoebe, R. Geer, C. C. Huang, and J. W. Goodby, Phys. Rev. Lett. **69**, 2090 (1992).
[12] R. Geer, T. Stoebe, T. Pitchford, and C. C. Huang, Rev. Sci. Instrum. **62**, 415 (1991).
[13] T. Stoebe, C. C. Huang, and J. W. Goodby, Phys. Rev. Lett. **68**, 2944 (1992).
[14] R. Geer, T. Stoebe, and C. C. Huang, Phys. Rev. E **48**, 408 (1993).
[15] T. Stoebe, Ph. D. thesis, University of Minnesota, 1993.
[16] R. Geer, T. Stoebe, C. C. Huang, and J. W. Goodby, Phys. Rev. A **46**, R6162 (1992).
[17] M. Schick, in *Liquids at Interfaces*, edited by J. Charvolin, J. F. Joanny, and J. Zinn-Justin (Elsevier Science, 1990) and references therein.